J. Phys. Chem. A **1999,** *103,* 451−459

ARTICLES

First Determination of the Branching Ratios between Reactive Removal and Vibrational Relaxation in Collisions of OH($X^2\Pi_i$, $v = 1$ and 2) with CH_4

Katsuyoshi Yamasaki,* Akihiro Watanabe,[†] Teruaki Kakuda,[‡] Noriko Ichikawa, and Ikuo Tokue

Department of Chemistry, Niigata University, Ikarashi, Niigata 950-2181, Japan

Received: May 27, 1998; In Final Form: September 14, 1998

Absolute rate constants for reactive removal and vibrational relaxation have been determined for the collisions of OH($X^2\Pi_i$, $v = 1$ and 2) with CH_4. The hydroxyl radical was produced in the reaction $O(^1D) + CH_4 \rightarrow OH(X^2\Pi_i, v \le 4) + CH_3$ initiated by the 248 nm photolysis of O_3 in the presence of CH_4. All the vibrational levels of OH(v) were detected by laser-induced fluorescence (LIF) via the sequences $\Delta v = 0$ ($v'' = 0$, 1, and 2) and $\Delta v = -3$ ($v'' = 3$ and 4) of the $A^2\Sigma^+-X^2\Pi_i$ transition. Temporal profiles of the LIF intensities were analyzed using a new linear regression method (refs 10 and 11), and total removal rate constants for the vibrational levels ($v = 1-4$) were determined. The linear analysis coupled with the previously reported nascent vibrational distributions of OH gave absolute rate constants for the reactive and nonreactive removal of OH(v). Rate constants for reactive removal, $OH(v) + CH_4 \rightarrow$ products, were determined to be $k(v{=}1) = (2.1 \pm 0.6) \times 10^{-13}$ cm^3 molecule^{-1} s^{-1} and $k(v{=}2) = (0.9 \pm 0.4) \times 10^{-12}$ cm^3 molecule^{-1} s^{-1}, and for vibrational relaxation, $OH(v) + CH_4 \rightarrow OH(v-1) + CH_4$, are $k(1{\rightarrow}0) = (3.5 \pm 0.6) \times 10^{-13}$ cm^3 molecule^{-1} s^{-1} and $k(2{\rightarrow}1) = (1.1 \pm 0.4) \times 10^{-12}$ cm^3 molecule^{-1} s^{-1}. This article is the first report on the branching ratios between reactive removal and vibrational relaxation.

1. Introduction

The hydroxyl radical (OH) is one of the most important species in combustion and atmospheric chemistry[1,2] because OH is involved in various radical chain reactions. For example, the HO_x cycle of ozone depletion in the stratosphere and the oxidation of hydrocarbons in the troposphere are initiated and propagated by OH.[3] Because CH_4 is more highly concentrated in the atmosphere than other hydrocarbons,[4] the reaction of OH with CH_4 has attracted the attention of many researchers engaged in atmospheric chemistry. There have been many reports on the rate constants of the reaction OH + CH_4 over a wide range of temperatures,[1,2] and a recommended value has been given to be $2.65 \times 10^{-12} \exp[(-15 \pm 1\ \text{kJ mol}^{-1})/(RT)]$ cm^3 molecule^{-1} s^{-1} (230 K $\le T \le$ 400 K).[2] The rate constant at 298 K is 6.3×10^{-15} cm^3 molecule^{-1} s^{-1}. Because there is an activation barrier, the vibrational excitation of reactants may accelerate the reaction. There are several possible reactive removals, as shown in reactions 1a−1i, and vibrational relaxations (reaction 2) in collisions of vibrationally excited OH(v) with CH_4.

$$OH(v) + CH_4 \rightarrow CH_3 + H_2O \qquad \Delta H = -60\ \text{kJ mol}^{-1} \tag{1a}$$

$$\rightarrow CH_3OH + H \qquad \Delta H = +52\ \text{kJ mol}^{-1} \tag{1b}$$

$$\rightarrow CH_3O + H_2 \qquad \Delta H = +53\ \text{kJ mol}^{-1} \tag{1c}$$

$$\rightarrow HCO + 2H_2 \qquad \Delta H = +78\ \text{kJ mol}^{-1} \tag{1d}$$

$$\rightarrow H_2CO + H_2 + H \qquad \Delta H = +145\ \text{kJ mol}^{-1} \tag{1e}$$

$$\rightarrow CH + H_2O + H_2 \qquad \Delta H = +388\ \text{kJ mol}^{-1} \tag{1f}$$

$$\rightarrow CH_2 + H_2O + H \qquad \Delta H = +401\ \text{kJ mol}^{-1} \tag{1g}$$

$$\rightarrow CH_3 + H_2 + O \qquad \Delta H = +432\ \text{kJ mol}^{-1} \tag{1h}$$

$$\rightarrow CH_3 + OH + H \qquad \Delta H = +439\ \text{kJ mol}^{-1} \tag{1i}$$

$$\rightarrow OH(v-1) + CH_4 \tag{2}$$

The heats of reaction shown for reactive processes 1a−1i represent the enthalpy changes for OH($v = 0$). The vibrational energies of OH(v) are 43, 83, 122, and 159 kJ mol^{-1} for $v = 1$, 2, 3, and 4, respectively; therefore, there is a possibility that reactions 1b−1e are open when the vibrational energies are larger than the endothermicities, although there might be higher activation barriers than the heats of reactions. The reaction

---

* To whom correspondence should be addressed. Fax: +81 25 262 7530. E-mail: yam@scux.sc.niigata-u.ac.jp.

[†] Department of Applied Chemistry, Kobe City College of Technology, Gakuen-Higashi-machi, Nishi-ku, Kobe 651-2194, Japan.

[‡] NIKKI CHEMCAL CO., LTD, Takiya-hon-cho, Niitsu, Niigata 956-0855, Japan.

10.1021/jp982392q CCC: $18.00

products were not identified in the present study, and we shall henceforth write "products" for the possible reaction products. Reactive removal is important in the initiation or propagation of chain reactions; on the other hand, relaxation just transfers the vibrational energy of OH to CH_4.

Overall rate constants for several vibrational levels have been reported,[5−9] although there has been no report of ratios between reactive removal and vibrational relaxation. The kinetics of vibrationally excited states can only be made clear by overall (total removal) rate constants together with the branching ratios. An excited vibrational level of interest simultaneously undergoes reaction and relaxation in collisions with ambient molecules. Even if the time-dependent profiles of vibrational populations are monitored, the branching ratio cannot be determined without calibration of the detectivities of the levels. Precise photochemical factors are usually needed to estimate the detectivities of different vibrational levels. Furthermore, experimental conditions, e.g., undesirable saturation or multiphoton process in photoabsorption, must be taken into account in the analysis. The difficulty of this kind of correction has prevented the determination of branching ratios between reaction and relaxation.

In the present study, we have applied a kinetic linear analysis, which has recently been developed by the authors' laboratory,[10,11] to analyze the temporal profiles of concentrations on the vibrational levels observed in arbitrary units. The analysis can derive overall rate constants even when the profiles of interest do not show a single- or double-exponential analytical form. If the relative detectivities of vibrational levels are determined, overall rate constants can be divided into the contributions of reaction and relaxation (Appendix). Fortunately, the nascent vibrational distributions of OH produced in the reaction $O(^1D) + CH_4$ have been reported by several previous studies,[6,12−14] and consequently, the branching ratios between reaction and relaxation have been obtained by the present analysis. It has been found that vibrational excitation of OH enhances reactive removal, and reported vibrational distributions of high vibrational levels ($v \geq 3$) are inconsistent with the present study.

2. Experimental Section

Because the experimental apparatus used in the present study has been described in detail elsewhere,[15] only the significant features of the present study are described here. Instantaneous preparation of vibrationally excited OH is preferred in studying the following kinetics of OH in collisions with CH_4. Molecules emitting OH in the photolysis, e.g., H_2O_2 and $HONO_2$, are candidates as parent molecules; however, vibrational levels higher than $v'' = 1$ are not effectively produced in these photolyses.[16,17] Reactions by which OH is produced as a new chemical bond are more appropriate for the production of vibrationally excited OH. In the present study, a reaction $O(^1D) + CH_4 \rightarrow OH + CH_3$ ($\Delta H = -179$ kJ mol^{-1}) was adopted to prepare vibrationally excited OH. The highest vibrational level is $v = 4$ if the exothermicity of the reaction is deposited only on OH.

A flow of the mixture of O_3 and CH_4 was irradiated with a 248 nm beam from a KrF laser (Lambda Physik LEXtra 50, 2 mJ cm^{-2} in the flow cell). Electronically excited oxygen $O(^1D)$ was produced in the photolysis followed by the reaction $O(^1D) + CH_4 \rightarrow OH(X^2\Pi_i, v = 0-4) + CH_3$. As stated above, because the OH should be prepared instantaneously, N_2 at 5 Torr was used as a carrier gas to accelerate the production rate of OH. Nitrogen is an effective quencher of $O(^1D)$ to $O(^3P)$, $k = 2.6 \times 10^{-11}$ cm^3 molecule^{-1} s^{-1},[2] and the $O(^3P)$ reacts with CH_4 much more slowly than $O(^1D)$, $k(298\text{ K}) = 5.0 \times 10^{-18}$ cm^3 molecule^{-1} s^{-1} and 1.5×10^{-10} cm^3 molecule^{-1} s^{-1} for $O(^3P)$[1] and $O(^1D)$,[2] respectively. A short time constant for the production of OH (0.2 μs) is achieved under the present experimental conditions, although about 70% of the $O(^1D)$ was quenched to $O(^3P)$ by N_2 under typical experimental conditions ($P_{CH_4} = 400$ mTorr, $P_{N_2} = 5$ Torr).

The pressure of O_3 was kept as low as possible because an unexpected secondary reaction 4 also produces vibrationally excited OH, and vibrational distributions of OH initially prepared by $O(^1D) + CH_4$ are perturbed.

$$O(^1D) + CH_4 \rightarrow OH(v \leq 4) + CH_3 \tag{3a}$$

$$\rightarrow CH_3O + H \tag{3b}$$

$$\rightarrow O(^3P) + CH_4 \tag{3c}$$

$$H + O_3 \rightarrow OH(v = 5-9) + O_2 \tag{4}$$

To reduce the effect of reaction 4, the pressure of ozone was lowered to 0.5 mTorr. The recommended branching ratios of reactions 3a−3c are (reaction 3a)/(reaction 3b)/(reaction 3c) = (75 ± 15%)/(20 ± 7%)/(5 ± 5%),[2] and the rate constant of reaction 4 is 2.9×10^{-11} cm^3 molecule^{-1} s^{-1} at 298 K.[2] The fraction of OH produced by reaction 4 was estimated to be at most 0.2% of OH by reaction 3a; thus, the effect of reaction 4 could be neglected in the present study.

Vibrationally excited $OH(X^2\Pi_i)$ was detected by laser-induced fluorescence (LIF) via $OH(A^2\Sigma^+-X^2\Pi_i)$ transitions using a frequency-doubled dye laser (Lambda Physik LPD-3002 with BBO crystal) pumped by a Nd^{3+}:YAG laser (Continuum YG660-20 or Spectron SL803). A sequence with $\Delta v = 0$ was used for probing the levels $v'' = 0$, 1, and 2. Because efficient predissociation occurs on all the rotational levels of $OH(A^2\Sigma^+, v' \geq 3)$[18,19] and fluorescence yields are very low for the levels $v' = 3$ and 4, a sequence with $\Delta v = -3$ was excited to detect $v'' = 3$ and 4. The photolysis and probe lasers were counter-propagated and overlapped in the flow cell, and the LIF was collected with a lens ($f = 80$ mm) and detected with a photomultiplier (Hamamatsu R374 or R1104) mounted perpendicularly to the laser lights. Recorded LIF excitation spectra of $OH(A^2\Sigma^+-X^2\Pi_i)$ $v'' = 0$, 1, and 2 ($\Delta v = 0$) and $v'' = 3$ and 4 ($\Delta v = -3$) are shown in Figures 1 and 2. Saturation occurred in the $\Delta v = 0$ sequence because the typical probe laser power was 100 μJ pulse^{-1}, and the $\Delta v = 0$ sequence is easily saturated at about 10 μJ pulse^{-1}.[20] The present method of analysis, however, is not affected at all by either predissociation or saturation.[10,11]

The signal from the photomultiplier tube (PMT) was averaged with a gated integrator (Stanford Research SR250) and stored on a computer. Temporal profiles of vibrational levels of interest were observed by the scan of the delay time between the photolysis and the probed laser. The rotational lines excited to record the temporal profiles were $P_1(2)$, $P_1(2)$, $Q_1(2)$, $Q_1(3)$, and $Q_1(2)$ of 0−0, 1−1, 2−2, 0−3, and 1−4 bands, respectively. Because the relaxation of rotational motion is much faster than that of vibration,[21] the time dependence of a single rotational line represents that of a single vibrational level. The typical number of data points in a profile was 2000, and the step size was 0.25 μs. Two or three profiles were recorded for a single vibrational level, and averaged signals were used in the analysis.

Flow rates of all the sample gases were controlled with calibrated mass flow controllers (Tylan FC-260 and STEC SEC-

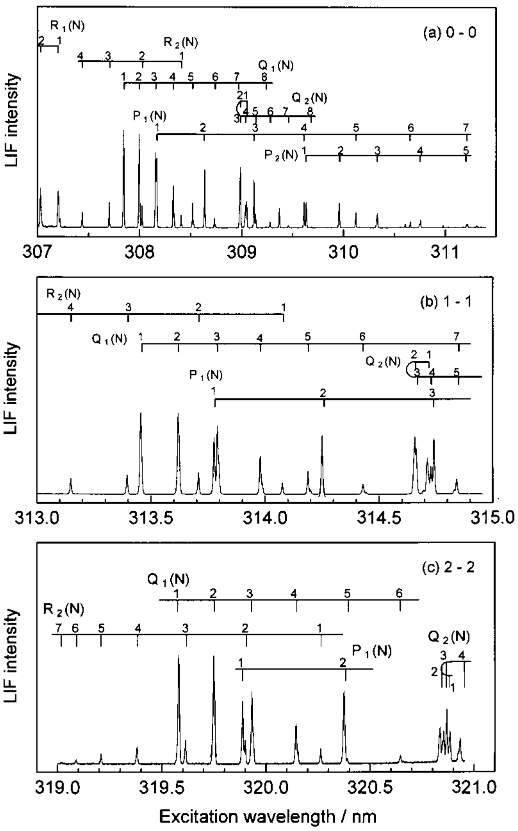

Figure 1. Laser-induced fluorescence excitation spectra of OH($X^2\Pi_i$, $v = 0$, 1, and 2) produced in the O(^{1}D) + CH_4 reaction. The fluorescence was excited via the $\Delta v = 0$ sequence: 0−0 (a); 1−1 (b); 2−2 (c). Delay times between the photolysis and probe lasers were 200 μs (a), 50 μs (b), and 25 μs (c).

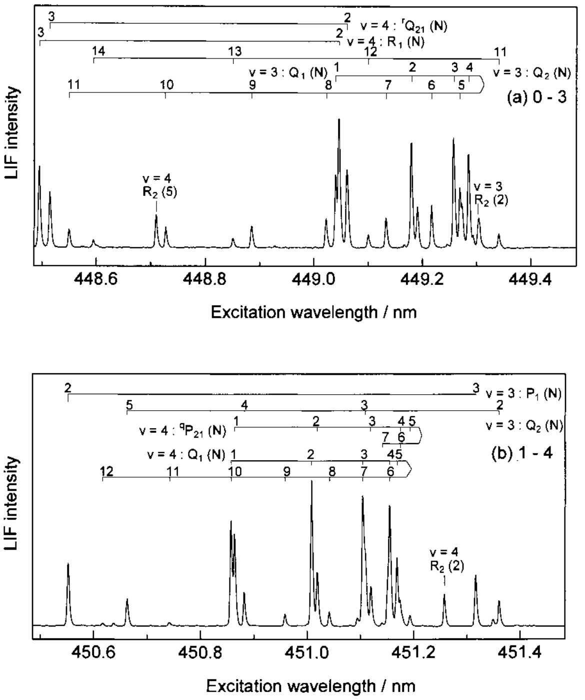

Figure 2. Laser-induced fluorescence excitation spectra of OH($X^2\Pi_i$, $v = 3$ and 4) produced in the O(^{1}D) + CH_4 reaction. The fluorescence was excited via the $\Delta v = -3$ sequence: 0−3 (a); 1−4 (b). Delay times between the photolysis and probe laser were 3 μs in both spectra.

400 mark3), and the linear velocity of the flow was 1 m s^{-1}. Total pressure in the flow cell was measured with a capacitance manometer (Baratron 122A), and a typical total pressure was 5 Torr to suppress the loss of species from the region of probed volume. The total pressure measurement together with the mole fractions as measured by the flow controllers gave the partial pressures of the reagents. Methane at pressures higher than 300 mTorr was added to distinguish between the production and relaxation in the rises of the signals of the levels $v \leq 3$. Because the highest level $v = 4$, to which no vibrational levels relax, showed a single-exponential decay, signals at lower pressures of CH_4 (100 mTorr < P_{CH_4}) were also observed. Ozone was prepared by electric discharge in pure oxygen (Toyo-Sanso, 99.9995%) with a homemade synthesizer and stored in a 3 dm^{-3} bulb with N_2 (1% dilution).

3. Results and Discussion

A. Overall Reaction Rate Constants. The temporal profiles of OH at 338 mTorr of CH_4 are shown in Figure 3. The reactions initiated by the photolysis of ozone in the presence of CH_4 are written as follows:

$$O(^1D) + CH_4 \rightarrow OH(v) + CH_3 \quad (5)$$

$$OH(v) + OH(v') \rightarrow OH(v + 1) + OH(v' - 1) \quad (6)$$

$$OH(v) + O_3 \rightarrow \text{products} \quad (7)$$

$$OH(v) + N_2 \rightarrow OH(v - 1) + N_2 \quad (8)$$

$$OH(v) + CH_4 \rightarrow \text{products} \quad (9)$$

$$OH(v) + CH_4 \rightarrow OH(v - 1) + CH_4 \quad (10)$$

$$OH(v) \rightarrow \text{diffusion} \quad (11)$$

The rate constant of reaction 5 is 1.5×10^{-10} cm^3 $molecule^{-1}$ s^{-1},[2] and the production of OH is therefore significantly faster than the following processes with CH_4 higher than 300 mTorr in the present experiment. Teitelbaum[22] has reported that the V−V energy transfer of OH (reaction 6) has a near-gas-kinetic rate. They also found that the rate constants for reaction or relaxation with O_3 (reaction 7) increase with the vibrational quantum number v (1.0×10^{-12} cm^3 $molecule^{-1}$ s^{-1} for v = (1−1.4) $\times 10^{-11}$ cm^3 $molecule^{-1}$ s^{-1} for $v = 4$). The concentration of initially prepared OH was estimated using the known photoabsorption cross section of O_3 at 248 nm ($\lambda = 1.08 \times 10^{-17}$ cm^2),[2] the known O(^{1}D) quantum yield (ϕ = 90%),[2] the laser energies (2 mJ $pulse^{-1}$), and the typical concentrations of CH_4 and N_2 in the experiments. The fractions of reactions 6 and 7 were estimated to be about 0.3% and 0.5% of all the processes of OH(v) because of concentrations of OH and O_3 that are lower than those of CH_4 in the present experiments. Processes 6 and 7, therefore, could be neglected in the analysis.

There have been few reports providing evidence of OH relaxation in the presence of N_2. Rensberger et al.[7] tried to measure the rate constant for the relaxation of OH($v = 2$) by N_2; however, they did not observe apparent relaxation and gave an upper limit of $<10^{-14}$ cm^3 $molecule^{-1}$ s^{-1}. Knutsen et al.[23] and Chalamala and Copeland[24] have reported that the rate constant for relaxation by N_2 is not significantly different from zero even for the levels $v = 7$ and 9 and have shown only the upper limits of $<6 \times 10^{-13}$ and $<5 \times 10^{-13}$ cm^3 $molecule^{-1}$ s^{-1} for $v = 7$ and 9, respectively. However, the rate of relaxation by N_2 (reaction 8) estimated using the upper limit of 10^{-14} cm^3 $molecule^{-1}$ s^{-1} at 5 Torr of N_2 is 3200 s^{-1}, which cannot be

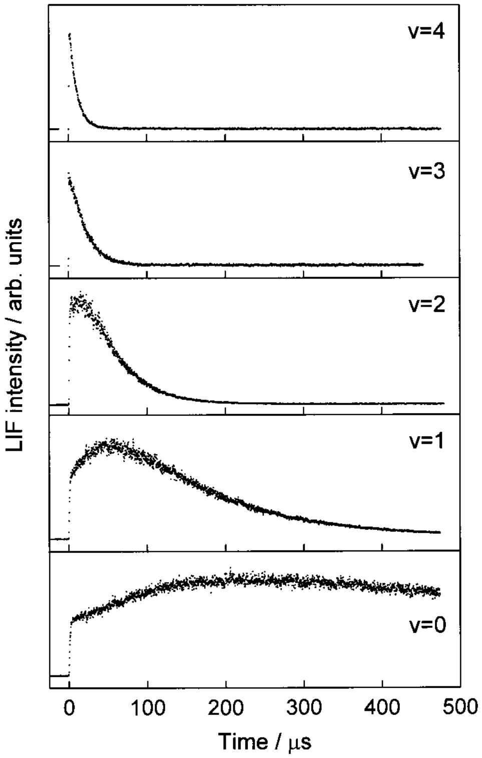

Figure 3. Temporal profiles of OH($X^2\Pi_i$, $v = 0-4$) produced in the reaction O(^{1}D) + CH_4. The abscissa corresponds to the delay time between the photolysis and probe lasers. The step size of the delay scan was 0.25 µs. The partial pressure of CH_4 was 338 mTorr, O_3 was 0.5 mTorr, and total pressure (buffer = N_2) was 5 Torr.

considered negligible in the analysis. The reaction of OH($v = 0$) with CH_4, for which the time constants were estimated to be 14 ms, was much slower than the observed decay rate of $v = 0$. No dependence of the decay rate of $v = 0$ on the CH_4 pressure was actually observed in the experiment. The level $v = 0$ decayed more slowly with higher total pressure, and thus, the decay of $v = 0$ resulted from diffusion out of the probed volume rather than from the reactions.

As seen in the temporal profiles of OH(v), the decay of upper vibrational levels corresponds to the growth of the lower levels after the prompt production of OH in the O(^{1}D) + CH_4 reaction. The phenomenon indicates that vibrational relaxation occurs on each level. The rate equations for the scheme having both reactive removal and vibrational relaxation under pseudo-first-order conditions [OH] ≪ [CH_4], [N_2] are expressed as follows:

$$\frac{d[\mathrm{OH}(v=4)]}{dt} = -\{(k_{43} + k_4)[\mathrm{CH_4}] + k_{43}^{\mathrm{N_2}}[\mathrm{N_2}] + k_d\}[\mathrm{OH}(v=4)] \quad (12)$$

$$\frac{d[\mathrm{OH}(v)]}{dt} = \{k_{v+1,v}[\mathrm{CH_4}] + k_{v+1,v}^{\mathrm{N_2}}[\mathrm{N_2}]\}[\mathrm{OH}(v+1)] - \{(k_{v,v-1} + k_v)[\mathrm{CH_4}] + k_{v,v-1}^{\mathrm{N_2}}[\mathrm{N_2}] + k_d\}[\mathrm{OH}(v)], \quad v = 1-3 \quad (13)$$

$$\frac{d[\mathrm{OH}(v=0)]}{dt} = \{k_{10}[\mathrm{CH_4}] + k_{10}^{\mathrm{N_2}}[\mathrm{N_2}]\}[\mathrm{OH}(v=1)] - k_d[\mathrm{OH}(v=0)] \quad (14)$$

where $k_{v+1,v}$ and $k_{v,v-1}$ are the second-order rate constants for vibrational relaxation from $v + 1$ to v and from v to $v - 1$ in collision with CH_4, k_v is a rate constant for reactive removal by CH_4, $k^{N_2}_{v+1,v}$ and $k^{N_2}_{v,v-1}$ are the rate constants for vibrational relaxation by N_2, and k_d is the first-order rate constant for the diffusion loss. Here, the rate of diffusion is assumed to be the same for all vibrational levels. This assumption is reasonable for vibrational relaxation because all the levels have the same mass and must have nearly the same diffusion rates.[25] Reactive removal of $v = 0$, k_0, is neglected because the calculated time constant of OH($v = 0$) + CH_4 is much longer than the observed time scales, and the decay rates of $v = 0$ were independent of CH_4 pressures.

In the present experiment, LIF intensities instead of concentrations of vibrational levels were recorded. Although absolute concentrations could not be measured, the LIF intensity observed was proportional to the concentration of each vibrational level, and the following equation was satisfied:

$$I_v(t) = \alpha_v[\mathrm{OH}(v)]_t \quad (15)$$

where $I_v(t)$ and α_v are the observed signal intensity at time t and the detectivity for a vibrational level v. After the absolute concentrations at time t, $[\mathrm{OH}(v)]_t$, in eqs 12−14 are replaced with eq 15, the following expressions are obtained:

$$I_4(t) = I_4(t_0) - \{(k_{43} + k_4)[\mathrm{CH_4}] + k_{43}^{\mathrm{N_2}}[\mathrm{N_2}] + k_d\}\int_{t_0}^{t} I_4(t')\,dt' \quad (16)$$

$$I_v(t) = I_v(t_0) + \frac{\alpha_v}{\alpha_{v+1}}\{k_{v+1,v}[\mathrm{CH_4}] + k_{v+1,v}^{\mathrm{N_2}}[\mathrm{N_2}]\}\int_{t_0}^{t} I_{v+1}(t')\,dt' - \{(k_{v,v-1} + k_v)[\mathrm{CH_4}] + k_{v,v-1}^{\mathrm{N_2}}[\mathrm{N_2}] + k_d\}\int_{t_0}^{t} I_v(t')\,dt' \quad (v = 1-3) \quad (17)$$

$$I_0(t) = I_0(t_0) + \frac{\alpha_0}{\alpha_1}\{k_{10}[\mathrm{CH_4}] + k_{10}^{\mathrm{N_2}}[\mathrm{N_2}]\}\int_{t_0}^{t} I_1(t')\,dt' - k_d\int_{t_0}^{t} I_0(t')\,dt' \quad (18)$$

It should be noted that all the equations are linear: $I_v(t)$ ($v = 0-4$) are dependent variables, and the integrals are independent variables. The integrated values were obtained by a numerical integration using a trapezoidal formula from time t_0 to t, where t_0 is not necessarily 0.[10,11] In principle, eqs 16−18 are satisfied for arbitrary t_0 to t. In the actual analysis, regression calculations were performed for at least 100 combinations of t_0 and t, and the regression coefficients obtained were averaged over all the combinations. The apparent first-order decay rate constants, $(k_{v,v-1} + k_v)[\mathrm{CH_4}] + k^{\mathrm{N_2}}_{v,v-1}[\mathrm{N_2}] + k_d$ ($v = 1-4$), were determined by the multilinear regression analyses using eqs 16 and 17. The overall rate constants $k_{v,v-1} + k_v$ for OH(v) + CH_4 reactions were determined from the plots of the first-order decay rates versus CH_4 pressures as shown in Figure 4, and the values are listed in Table 1. The small intercepts seen in Figure 4 can be ascribed to the relaxation by N_2 and the diffusion loss $k^{\mathrm{N_2}}_{v,v-1}[\mathrm{N_2}] + k_d$. The present analysis showed the relaxation by N_2, $k^{\mathrm{N_2}}_{v,v-1}$, to be within the range of 2×10^{-15} to 5×10^{-14} $\mathrm{cm^3\ molecule^{-1}\ s^{-1}}$, and the results are consistent with those of previous studies.[7,23,24]

There have been several reports of the overall rate constants for $v = 1$ and 2. The rate constant for $v = 1$ ($k_{10} + k_1$) obtained in the present study is in good agreement with reported values within the error limits. The values for $v = 2$ from the previous studies are somewhat scattered. Glass et al.[5] have produced OH($v \leq 2$) by the reaction H + NO_2 → OH + NO in a discharge

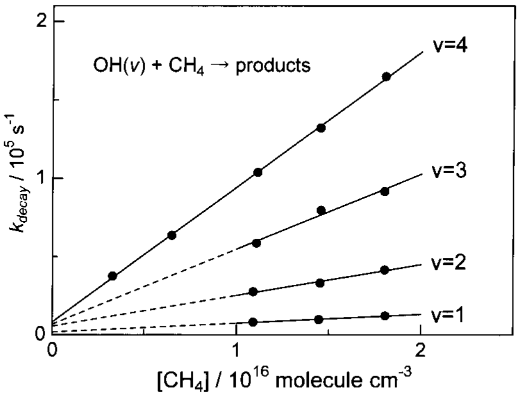

Figure 4. Methane pressure dependence of the first-order decay rates of OH(v) in collisions with CH_4. The straight lines show the results of a linear least-squares fit, and their slopes correspond to the overall rate constants $k_{v,v-1} + k_v$ for OH(v) + CH_4 (v = 1−4) reactions.

flow apparatus, detecting OH with an EPR spectrometer. They indirectly determined the rate constant for $v = 2$ using nitric oxide as the standard deactivator. They used an early rate constant 1.5×10^{-11} cm^3 molecule^{-1} s^{-1} for OH($v = 1$) + NO → OH($v = 0$) + NO reported by Jaffer and Smith;[26] however, Smith and Williams[27] revised the rate constant to be 3.8×10^{-11} cm^3 molecule^{-1} s^{-1}. Rate constants corrected by the newly recommended values are listed in Table 1. Steady-state analysis based on a variety of assumptions might explain the small difference from other studies.

Cheskis et al.[6] have photolyzed O_3 at 266 nm in the presence of CH_4 and detected vibrationally excited OH by LIF, which is similar to the system used in the present study. They analyzed the temporal profiles of OH(v) on the assumption that all the profiles were expressed by double exponentials. Strictly, the assumption was not correct. In general, the time dependence of the ith species in the following scheme

$$A_1 \xrightarrow{k_1} A_2 \xrightarrow{k_2} A_3 \xrightarrow{k_3} A_4 \ldots A_{i-1} \xrightarrow{k_{i-1}} A_i \xrightarrow{k_i} A_{i+1} \ldots \quad (19)$$

is given by the multiexponential equation[28]

$$[A_i] = C_{i1} \exp(-k_1 t) + C_{i2} \exp(-k_2 t) + \ldots + C_{i,i-1} \exp(-k_{i-1} t) + C_{ii} \exp(-k_i t) \quad (20)$$

where k_i is the first-order rate constant for the process shown in reacton 19 and the constants (C_{i1}, C_{i2}, ..., C_{ii}) are determined from the initial conditions. The profile of A_i is approximated to be double exponential in the temporal range over which the following inequality is satisfied:

$$\exp(-k_1 t), \exp(-k_2 t), \ldots, \exp(-k_{i-2} t) \ll \exp(-k_{i-1} t), \exp(-k_i t) \quad (21)$$

Here, an alternative quantitative condition is given: the right-hand side of eq 21 is at least 10 times as large as the left-hand side. Critical times, after which the double-exponential approximation is appropriate, can be defined. Under the typical experimental conditions ([CH4] = 10^{16} molecule cm^{-3}) of ref 6, the inequality is satisfactory after about 80 and 60 μs for v = 1 and v = 2, respectively. They are too late to apply the double-exponential approximation to both profiles. Furthermore, Cheskis et al. recorded only about 10 data points for each profile, and the number was too small to determine accurate rate constants. Their somewhat smaller rate constant for $v = 2$ might derive from the causes described above. Rensberger et al.[7] and Raiche et al.,[8] who belong to the same group, prepared OH(v = 2) by overtone excitation, observing the time evolution of v = 2 by LIF. They fitted the observed profiles to single exponentials and obtained overall rate constants. Their method was an ideal one for determining the overall rate constant of a single vibrational level. Their value agrees well with ours.

There has been only two reports on the total removal rate constant for $v = 3$. The value reported by Cheskis et al.[6] is about 1.5 times as large as those obtained by other studies. The large discrepancy might be due to too small number of data points for very fast growth and decay. Their value, however, overlaps with others because of their large error limits. All the values for v = 1−3 reported by Silvente et al.[9] are in remarkably agreement with ours. They first applied single-exponential analysis to the signals over late times and then performed multiparameter fitting. As pointed out by them, single-exponential analysis can be applied only when the rate of growth is sufficiently faster than that of decay. Analysis using the signals at longer reaction times derives more accurate decay rates; however, the signals over late times are weak and the signal-to-noise ratio is usually low. We have also analyzed our profiles using the single-exponential approximation, obtaining similar results with those obtained by the present integration method. The fact indicates that single-exponential analysis can be used for the present system. However, it should be noted that the present method is equivalent to the single-exponential analysis. All the first-order decay rates obtained by the single-exponential approximation were smaller than those obtained by the present integrated profiles method. The fact indicates that the effect of growth remains at long reaction times. Despite the *incorrect* first-order decay rates, bimolecular overall rate constants were fortunately obtained because they are given by the slopes of the plots. All the points plotted were shifted to lower values, and the slopes were not seriously affected. Therefore, the single-exponential approximation is not always safe to analyze the profiles with growth and decay, and the intercepts of the plots are meaningless. As for $v = 4$, the rate constant given in the present study is the first one to the best of our knowledge.

Shalashilin et al.[29] have performed trajectory calculations and have shown the predominance of one-quantum relaxation for low and multiquantum transitions for high OH vibrational levels in OH(v) + O_2 collisions. The present method can be applied to the schemes with not only $\Delta v = 1$ but also $\Delta v > 1$,[10,11] although the expressions are more complicated than eqs 16−18. For example, a term $(\alpha_{v-\Delta v}/\alpha_v)(k_{v,v-\Delta v}[CH_4] + k^{N_2}_{v,v-\Delta v}[N_2])$ is added to the equation of $I_v(t)$ when the Δv relaxation from v is in a scheme. Negligible values of the terms $(\alpha_{v-\Delta v}/\alpha_v)(k_{v,v-\Delta v}[CH_4] + k^{N_2}_{v,v-\Delta v}[N_2])$ with $\Delta v > 1$ were obtained from the analysis using all the possible relaxation processes ($1 \leq \Delta v \leq v$). The results indicate that the contributions of the multiquantum relaxation $\Delta v > 1$ can be negligible in OH(v) + CH_4.

In the previous paper,[11] we analyzed synthesized signals having artificial noises and demonstrated that the present method is not affected by random noise. Integration eliminates undesirable effects of the fluctuation of the signals. Integration curves $\int_{t_0}^{t} I_v(t')\,dt'$ vs t, for v = 1−4, smoothly converged to constant values, indicating that proper baselines were subtracted and that the real noise on the observed signals did not disturb the analysis.

B. Branching Ratios between Reactive Removal and Vibrational Relaxation. As shown in the previous section, the apparent decay rate constant, $(k_{v,v-1} + k_v)[CH_4] + k^{N_2}_{v,v-1}[N_2] + k_d$, was determined in the analysis of the profile of v ($I_v(t)$),

TABLE 1: Overall Rate Constants for the OH(v) + CH_4 Reactions[a]

$k_{43} + k_4$	$k_{32} + k_3$	$k_{21} + k_2$	$k_{10} + k_1$	ref
		$(1.3 \pm 0.3) \times 10^{-12\,b}$	$(5.2 \pm 0.7) \times 10^{-13\,b}$	5
	$(6.8 \pm 2.0) \times 10^{-12}$	$(1.5 \pm 0.4) \times 10^{-12}$	$(5.1 \pm 1) \times 10^{-13}$	6
		$(2.3 \pm 0.2) \times 10^{-12}$		7
		$(2.46 \pm 0.25) \times 10^{-12}$	$(5.03 \pm 1.26) \times 10^{-13}$	8
	$(4.49 \pm 0.20) \times 10^{-12}$	$(2.02 \pm 0.20) \times 10^{-12}$	$(5.06 \pm 0.40) \times 10^{-13}$	9
$(8.6 \pm 0.3) \times 10^{-12}$	$(4.8 \pm 0.4) \times 10^{-12}$	$(2.0 \pm 0.2) \times 10^{-12}$	$(5.6 \pm 0.7) \times 10^{-13}$	this work[c]

[a] Values are in units of cm^3 molecule^{-1} s^{-1}. Rate constants for vibrational relaxation and reactive removal by CH_4 are $k_{v,v-1}$ and k_v, respectively. [b] Values in ref 5 were corrected using a more reliable rate constant for the reference reaction. [c] Quoted errors are 2σ.

TABLE 2: Reported Nascent Vibrational Distributions of OH Produced in the Reaction O(^{1}D) + CH_4[a]

$v = 4$		$v = 3$		$v = 2$		$v = 1$		$v = 0$	ref
						1.00		1.00	12
							1.00		
0.52 ± 0.29^b		0.96 ± 0.15^b		1.22 ± 0.12^b		1.00 ± 0.15^b			13
	1.85 ± 1.07		1.27 ± 0.23		0.82 ± 0.14				
0.03		0.52		1.28		1.00		0.62	6
	17.3		2.46		0.78		0.62		
0.20		0.48		1.32		1.00		1.00	14
	2.40		2.75		0.76		1.00		

[a] Upper numbers in each row are nascent vibrational distributions normalized by the population of $v = 1$. Lower numbers are population ratios $P(v\text{-}1)/P(v)$. [b] Quoted errors were estimated from the root-mean-square (σ) noise amplitude in ref 13.

and its dependence on CH_4 pressures gave $k_{v,v-1} + k_v$ (slope) and $k^{N_2}_{v,v-1}[N_2] + k_d$ (intercept), as shown in Figure 4. The common diffusion rate constant k_d was obtained from the analysis using eq 18 for $v = 0$. On the other hand, the ratio of the detectivities times the relaxation rate constant, $(\alpha_{v-1}/\alpha_v)\{k_{v,v-1}[CH_4] + k^{N_2}_{v,v-1}[N_2]\}$, was obtained from the analysis of level $v - 1$ ($I_{v-1}(t)$). Therefore, if the ratios of detectivities, α_{v-1}/α_v, are given, vibrational relaxation rate constants, $k_{v,v-1}$, can be obtained, and as a result, the reactive removal rate constants, k_v, are determined. The ratios of detectivities are derived using the information on the nascent vibrational distributions of OH produced in the O(^{1}D) + CH_4 reaction. Mathematical details regarding how to calculate the ratios of detectivities are described in the Appendix.

There have been several reports on the nascent vibrational distributions of OH produced in the reaction O(^{1}D) + CH_4 → OH(v) + CH_3.[6,12−14] As shown in the Appendix, only the ratios of adjacent levels $P(v-1)/P(v)$ instead of absolute distributions on whole vibrational levels are necessary to derive $k_{v,v-1}$ and k_v. Reported distributions are listed in Table 2 along with the population ratios $P(v-1)/P(v)$. Unfortunately, confidence limits of the values are not quoted in most of the original papers. Luntz[12] and Park and Wiesenfeld[14] determined the distributions by the analysis of rotationally resolved LIF excitation spectra recorded under collision-free conditions for nascent OH. Cheskis et al.[6] analyzed temporal profiles of LIF using a kinetic analysis on the assumption that the reactive removal channel in OH(v) + CH_4 collisions was negligible. Aker and Sloan[13] observed infrared emission spectra of OH produced in O(^{1}D) + CH_4 using FTIR, and they reported distributions except for $v = 0$. Luntz[12] and Park and Wiesenfeld[14] reported the ratio of $P(0)/P(1)$ to be unity, and Cheskis et al. gave 0.62. We adopt unity as the population ratio $P(0)/P(1)$ by the following reasons: inefficient predissociation on $v' = 0$ and $v' = 1$ of OH($A^2\Sigma^+$) did not seriously disturb spectroscopic approaches, and the scheme without reactive removal used by Cheskis et al. is inconsistent with the present study. The ratios $P(1)/P(2)$ determined by infrared emission and UV LIF are close, and the averaged value of 0.79 was used in the present analysis. The ratios $P(2)/P(3)$ and $P(3)/P(4)$ of the literature values are widely different, and there are no recommended ratios.

TABLE 3: Rate Constants of Vibrational Relaxations and Reactive Removals for the OH(v) + CH_4 Reactions[a]

	$v = 2$	$v = 1$	$v = 0$
$k_{v,v-1}$	$(1.1 \pm 0.4) \times 10^{-12}$	$(3.5 \pm 0.6) \times 10^{-13}$	
k_v	$(0.9 \pm 0.4) \times 10^{-12}$	$(2.1 \pm 0.6) \times 10^{-13}$	$(6.3 \pm 0.6) \times 10^{-15\,b}$

[a] Rate constants for vibrational relaxations and reactive removal by CH_4 are $k_{v,v-1}$ and k_v, respectively. The values are in units of cm^3 molecule^{-1} s^{-1}. Quoted errors are 2σ. [b] Rate constant at 297 K recommended by NASA/JPL.[2]

Rate constants for reactive removal and vibrational relaxation of $v = 1$ and 2 resulting from the present analysis are listed in Table 3. The errors are mainly caused by the following factors: the fluctuation of the CH_4 pressure dependence of the term $k_{v,v-1}[CH_4]$, the dependence of the regression coefficients on the analyzed range (t_0 and t), and the difference of the reported population ratios $P(v-1)/P(v)$ and their errors.

First, the reactive removal of $v = 1$ is significantly accelerated: $k_1/k_0 = 33 \pm 10$ (2σ). Although the rates of $v = 2$ have large error bars, not only the relaxation but also the reaction is accelerated. The findings indicate that the vibrational excitation of OH is effective in opening reactive channels. An experimental activation energy for the reaction OH + CH_4 → CH_3 + H_2O is 15 ± 1 kJ mol^{-1},[2] and the energy of the first vibrational quantum is 42.7 kJ mol^{-1} (3568 cm^{-1}).[19] The OH($v = 1$) + CH_4 as a whole system, therefore, has an energy that is approximately 28 kJ mol^{-1} higher than the barrier. The excess energy along the reaction coordinate might be less than 28 kJ mol^{-1} because of vibrational energy randomization in $CH_4OH^‡$, whereas the present results show that OH excitation is effective in accelerating the reactive removal.

Cannon et al.[30] have reported that the overall rate constant for OH($v = 1$) + HBr, $(8.1 \pm 1.15) \times 10^{-12}$ cm^3 molecule^{-1} s^{-1}, is smaller than that for OH($v = 0$) + HBr, $(1.12 \pm 0.045) \times 10^{-11}$ cm^3 molecule^{-1} s^{-1}. Smith et al.[31] have found that total removal by HCl and DCl were not as enhanced by a single-quantum excitation of OH. These results suggest that the single-quantum excitation of OH does not enhance exothermic reactions with low activation energy.[7] However, the activation energies for OH + HBr and OH + HCl are 0 ± 2 and 2.9 ± 0.8 kJ mol^{-1},[2] and these values are much smaller than that for OH + CH_4, 15 ± 1 kJ mol^{-1}. Therefore, it can be concluded that no effects of vibrational excitation of OH on the reactions OH + HBr and OH + HCl were due to the small energy barriers and that the large effect on OH + CH_4 found in the present study is due to the relatively large activation energy.

The enhancement of the reaction OH + CH_4 by excitation of OH vibration is counterintuitive from the viewpoint of reaction dynamics because OH seems to be a spectator of the reaction. Ab initio calculations[32,33] have shown that the O−H bond in transition state CH_3−H−O−H is almost perpendicular to the C···O axis (98°). The length of the “old” OH bond of the transition state (0.97 Å) is nearly identical with that of H_2O in equilibrium (0.96 Å). Newly formed OH bond in CH_3−H−O−H, on the other hand, is much longer (1.28 Å[32] and 1.33 Å[33]) than another OH bond. This suggests that the vibration of the new OH bond in the product H_2O might be highly excited, and consequently, the antisymmetric stretching vibration of H_2O can be excited. It is therefore not surprising that the excitation of OH vibration correlating with the H_2O antisymmetric vibrational motion enhances the reactive process.

It is difficult to determine the branching ratios for OH($v = 3$) + CH_4 and OH($v = 4$) + CH_4 because there are no highly reliable values of the population ratios $P(2)/P(3)$ or $P(3)/P(4)$. The calculated rate constant for vibrational relaxation $k_{v,v-1}$ became large when a large population ratio $P(v-1)/P(v)$ was used. Rate constant k_{32} was calculated to be 5.7×10^{-12} cm^3 $molecule^{-1}$ s^{-1} using $P(2)/P(3) = 1.27$ from ref 13 and 1.3×10^{-11} cm^3 $molecule^{-1}$ s^{-1} using $P(2)/P(3) = 2.75$ from ref 14. Both are too large because the magnitude of k_{32} must be that of the overall rate constant ($k_{32} + k_3 = 4.8 \times 10^{-12}$ cm^3 $molecule^{-1}$ s^{-1}) or less. Inversely, a tentative value of $P(2)/P(3)$ was calculated to be 0.78 on the assumption that $k_{32}/(k_{32} + k_3) = 0.7$. Aker and Sloan[13] reported that their result on OH vibrational distribution was a lower limit because they did not observe signals at sufficiently low pressures. Accordingly, there is a possibility that a correct distribution is “hotter” than theirs, and the value of $P(2)/P(3)$ is lower than 1.27. Park and Wiesenfeld[14] observed rotationally resolved LIF excitation spectra of OH($v \geq 2$) using off-diagonal ($\Delta v \neq 0$) sequences to prevent predissociation in the excited state. However, relative Einstein coefficients for off-diagonal sequences are very low, e.g., $A_{03}/A_{00} = 5.7 \times 10^{-6}$,[34] indicating that accurate populations of higher vibrational levels are difficult to determine. Copeland et al.[34] have given the absolute Einstein coefficients for the transitions $A_{v'v''}$($v' = 0$, 1 and $v'' = 0-4$). Of these, A_{03} was given to be 9 ± 6 (2σ) s^{-1}, with the error being too large for quantitative studies. As for $v = 4$, $k_{43} = 5.1 \times 10^{-12}$ cm^3 $molecule^{-1}$ s^{-1} was obtained by $P(3)/P(4) = 1.85$ from ref 13, and $k_{43} = 6.7 \times 10^{-12}$ cm^3 $molecule^{-1}$ s^{-1} was derived using $P(3)/P(4) = 2.40$ from ref 14. It must, however, be said that the values of k_{43} are also tentative because the accuracy of $P(3)/P(4)$ relies partly on that of $P(2)/P(3)$.

Cheskis et al.[6] has concluded that reactive removal of OH(v) by CH_4 is negligible. This is in marked contrast to the present study. They have measured total OH($v = 0$) yields with and without an effective relaxer H_2O. They found no significant difference between them. However, it should be noted that this type of measurement is not necessarily quantitative because added molecules change not only the reaction schemes but also the photochemical conditions of detection. They added H_2O of 3×10^{15} molecule cm^{-3} to the system. The fluorescence lifetime of OH($A^2\Sigma^+$, $v = 0$) without H_2O is estimated to be 110 ns using the radiative lifetime of OH($A^2\Sigma^+$, $v = 0$), 720 ns,[19] and using the quenching rate constant of CH_4, 2.6×10^{-10} cm^3 $molecule^{-1}$ s^{-1}.[35] When H_2O was added, the lifetime was reduced to about 85 ns because H_2O quenches OH($A^2\Sigma^+$, $v = 0$) about 3 times as effectively as CH_4.[35] The addition of H_2O reduced a fluorescence yield by about 30% when the amount of added H_2O was only 10% of that of CH_4. The decrease in the fluorescence lifetime might change the conditions of overlap between fluorescence decay curves and the gate of the boxcar integrator.

We have estimated the change of the LIF intensity of $v = 0$ by the addition of H_2O ($[H_2O]/[CH_4] = 10$) using the rate constants obtained in the present study. It was assumed that $k_{v,v-1}/(k_{v,v-1} + k_v) = 0.7$ for $v = 3$ and 4. The rate constant for $v = 4$ by OH is not available, and $k_{43}^{H_2O}$ was assumed to be 1.4×10^{-10} cm^3 $molecule^{-1}$ s^{-1} ($=2k_{32}^{H_2O}$). Although the increase of the OH($v = 0$) yield was calculated to be about 60%, detectivity decreased by about 25% because of the quenching of OH by H_2O. As a result, the expected increment of the LIF intensity was only about 20%. The change of the overlap of the detection gate and signals was not taken into account in the estimation. The calculation indicates that an expected increase in LIF intensity based on the growth of the concentration is considerably offset by the electronic quenching. Unfortunately, Cheskis et al.[6] did not show their data or the size of errors, and it is unclear how they reached the conclusion. If much more H_2O is added to the system to see the significant acceleration of relaxation by H_2O, photochemical parameters would be largely changed and complicated corrections would be needed to evaluate the correct intensities of LIF. Therefore, the measurement of the signal intensities with and without added molecules (H_2O) does not lead to a decisive conclusion for the contribution of the reactive removal.

4. Summary

A new kinetic analysis developed by the authors has first been applied to determine the overall rate constants for the reactions of vibrationally excited OH($X^2\Pi_i$, $v = 1-4$) with CH_4. Problems of nonlinear least-squares fit can be circumvented by the analysis. The method is also useful for determining the branching ratios between reactive removal and vibrational relaxation if initially prepared vibrational distributions are available.

The significant findings of this study are that even a single-quantum excitation of the OH vibration effectively accelerates the reactive removal of OH by CH_4. The present study predicts that the nascent population of OH($v = 3$) in the reaction O(^1D) + CH_4 should be higher than the values reported so far.

Acknowledgment. The authors are grateful for their fruitful discussions with Mr. Manabu Sato and Mr. Akira Itakura. This work was supported by “Free Radical Science”, the Grant-in-Aid for Scientific Research on Priority Areas (Contract No. 05237106), a Grant-in-Aid for Scientific Research (B) (Contract No. 08454181), and a Grant-in-Aid for Scientific Research (C) (Contract No. 10640486) of the Ministry of Education, Science, Sports, and Culture.

Appendix

How to determine the branching ratios between reactive removal and vibrational relaxation is described in this appendix. The analysis using eqs 16−18 in the text gives the rate constants $k_{v,v-1} + k_v$ and $k_{v,v-1}^{N_2}[N_2]$ and coefficients $(\alpha_{v-1}/\alpha_v)\{k_{v,v-1}[CH_4] + k_{v,v-1}^{N_2}[N_2]\}$. The relative detectivities, α_{v-1}/α_v, are necessary to determine $k_{v,v-1}$ and k_v. There are two ways of evaluating the relative detectivities.

The first one is useful only when the signal intensities at $t = 0$ on time evolution are apparent. Let $I_v(t{=}0)$ and $I_{v-1}(t{=}0)$ be the observed intensities of the levels v and $v - 1$, respectively. As defined in eq 15 in the text, $I_v(t{=}0) = \alpha_v[v_0]$ and $I_{v-1}(t{=}0) = \alpha_{v-1}[v - 1]$ are satisfied, and the following equation is obtained:

$$\frac{\alpha_{v-1}}{\alpha_v} = \frac{I_{v-1}(t{=}0)}{I_v(t{=}0)}\frac{[v]_0}{[v-1]_0} \qquad \text{(A1)}$$

where $[\mathrm{OH}(v)]$ is simply represented by $[v]$. If the ratio of $[v]_0$ to $[v - 1]_0$ is known, the relative detectivity, α_{v-1}/α_v, can be determined. Since $[v]_0/[v - 1]_0$ is the ratio of the nascent population of v and $v - 1$, relative detectivities are obtained from the information on the nascent vibrational distributions.

However, there are many cases in which the signal intensities at $t = 0$ are not always clear on the profiles, particularly when the production is not sufficiently faster than the following reactions and/or relaxation. Even in such a case, relative detectivities can be determined on the basis of the technique similar to the integrated profiles method.[10,11] The initially prepared $O(^1D)$ is quenched by N_2 and converted to OH by CH_4, and the decay is expressed as single exponential

$$[O(^1D)] = [O(^1D)]_0 \exp(-k^0 t) \qquad \text{(A2)}$$

where k^0 is the first-order decay rate constant of $O(^1D)$, and $[O(^1D)]_0$ is the initial concentration of $O(^1D)$. The rate equation for OH in vibrational level v is

$$\frac{d[v]}{dt} = k_v^0[O(^1D)]_0 \exp(-k^0 t) + \{k_{v+1,v}[CH_4] + k_{v+1,v}^{N_2}[N_2]\}[v + 1] - \{(k_{v,v-1} + k_v)[CH_4] + k_{v,v-1}^{N_2}[N_2] + k_d\}[v] \qquad \text{(A3)}$$

To deal with signal intensities, absolute concentrations $[v]$ and $[v + 1]$ in eq A3 are replaced with signal intensities $I_v(t)$ and $I_{v+1}(t)$ in eq 15 in the text. After the substitution, eq A3 is written as a rate equation for signal intensities:

$$\frac{dI_v(t)}{dt} = \alpha_v k_v^0[O(^1D)]_0 \exp(-k^0 t) + \frac{\alpha_v}{\alpha_{v+1}}\{k_{v+1,v}[CH_4] + k_{v+1,v}^{N_2}[N_2]\}I_{v+1}(t) - \{(k_{v,v-1} + k_v)[CH_4] + k_{v,v-1}^{N_2}[N_2] + k_d\}I_v(t) \qquad \text{(A4)}$$

Because the concentration of the level v at $t = 0$ is zero, the following relation is satisfied for any vibrational level v:

$$\int_0^t \frac{dI_v(t')}{dt'}\,dt' = \int_0^t dI_v(t') = I_v(t) - I_v(0) = I_v(t) \qquad \text{(A5)}$$

The following equations are derived after the integration of eq A4 from $t = 0$ to arbitrary time t:

$$\frac{k_v^0\alpha_v[O(^1D)]_0}{k^0}[1 - \exp(-k^0 t)] = I_v(t) - \frac{\alpha_v}{\alpha_{v+1}}\{k_{v+1,v}[CH_4] + k_{v+1,v}^{N_2}[N_2]\}\int_0^t I_{v+1}(t')\,dt' + \{(k_{v,v-1} + k_v)[CH_4] + k_{v,v-1}^{N_2}[N_2] + k_d\}\int_0^t I_v(t')\,dt' \qquad \text{(A6)}$$

A similar equation is obtained for the level $v - 1$. Although eq A6 looks to be complicated, the coefficients, $(\alpha_v/\alpha_{v+1})\{k_{v+1,v}[CH_4] + k_{v+1,v}^{N_2}[N_2]\}$ and $(k_{v,v-1} + k_v)[CH_4] + k_{v,v-1}^{N_2}[N_2] + k_d$, and signal intensities at t, $I_{v+1}(t)$ and $I_v(t)$, are known at this stage. Consequently, the values of the right-hand side can be calculated with great ease. On the other hand, the ratio of the left-hand side for the levels $v - 1$ and v gives the following ratio:

$$\frac{k_{v-1}^0}{k_v^0}\frac{\alpha_{v-1}}{\alpha_v} \qquad \text{(A7)}$$

The value is calculated using the right-hand side of eq A6 for $v - 1$ and v. It should be noted that these equations are satisfied at any time t. Because the ratio k_{v-1}^0/k_v^0 in eq A7 corresponds to the nascent population ratio $P(v{-}1)/P(v)$, relative detectivities α_{v-1}/a_v can be determined if the nascent distributions of adjacent vibrational levels are given. Once the ratios α_{v-1}/a_v are obtained, $k_{v,v-1}$ and k_v can be readily determined. In the actual analysis, the values of the right-hand side of eq A6 at time t were averaged over more than 800 data points.

References and Notes

(1) Baulch, D. L.; Cobos, C. J.; Cox, R. A.; Esser, C.; Frank, P.; Just, Th.; Kerr, J. A.; Pilling, M. J.; Troe, J.; Walker, R. W.; Warnats, J. *J. Phys. Chem. Ref. Data* **1992**, *21*, 411.

(2) DeMore, W. B.; Sander, S. P.; Golden, D. M.; Hampson, R. F.; Kurylo, M. J.; Howard, C. J.; Ravishankara, A. R.; Kolb, C. E.; Molina, M. J. *Chemical Kinetics and Photochemical Data for Use in Stratospheric Modeling*; JPL Publication 94-26; Jet Propulsion Laboratory, California Institute of Technology: Pasadena, 1994.

(3) Crutzen, P. J. *Physics and Chemistry of Upper Atmospheres*; McCormac, B. M., Ed.; D. Reidel Publishing: Dordrecht, 1973.

(4) Heicklen, J. *Atmospheric Chemistry*; Academic Press: New York, 1976.

(5) Glass, G. P.; Endo, H.; Chaturvedi, B. K. *J. Chem. Phys.* **1982**, *77*, 5450.

(6) Cheskis, S. G.; Iogansen, A. A.; Kulakov, P. V.; Razuvaev, I. Yu.; Sarkisov, O. M.; Titov, A. A. C*hem. Phys. Lett.* **1989**, *155*, 37.

(7) Rensberger, K. J.; Jeffries, J. B.; Crosley, D. R. *J. Chem. Phys.* **1989**, *90*, 2174.

(8) Raiche, G. A.; Jeffries, J. B.; Rensberger, K. J.; Crosley, D. R. *J. Chem. Phys.* **1990**, *92*, 7258.

(9) Silvente, E.; Richter, R. C.; Hynes, A. J. *J. Chem. Soc., Faraday Trans.* **1997**, *93*, 2821.

(10) Yamasaki, K.; Watanabe, A. *Bull. Chem. Soc. Jpn.* **1997**, *70*, 89.

(11) Yamasaki, K.; Watanabe, A.; Kakuda, T.; Tokue, I. *Int. J. Chem. Kinet.* **1998**, *30*, 47.

(12) Luntz, A. C. *J. Chem. Phys.* **1980**, *73*, 1143.

(13) Aker, P. M.; O'Brien, J. J. A.; Sloan, J. J. *J. Chem. Phys.* **1986**, *84*, 745.

(14) Park, C. R.; Wiesenfeld, J. R. *J. Chem. Phys.* **1991**, *95*, 8166.

(15) Yamasaki, K.; Tanaka, A.; Watanabe, A.; Keiichi, Y.; Tokue, I. *J. Phys. Chem.* **1995**, *99*, 15086.

(16) Ondrey, G. S.; van Veen, N.; Bersohn, R. *J. Chem. Phys.* **1983**, *78*, 3732.

(17) Jacobs, A.; Kleinermanns, K.; Kuge, H.; Wolfrum, J. *J. Chem. Phys.* **1983**, *79*, 3162.

(18) Heard, D. E.; Crosley, D. R.; Jeffries, J. B.; Smith, G. P.; Hirano, A. *J. Chem. Phys.* **1992**, *96*, 4366.

(19) Huber, K. P.; Herzberg, G. *Molecular Spectra and Molecular Structure, IV. Constants of Diatomic molecules*; Van Nostrand Reinhold: New York, 1979.

(20) Honma, K. *J. Chem. Phys.* **1993**, *99*, 7677.

(21) Levin, R. E.; Bernstein, R. B. *Molecular Reactions and Chemical Reactivity*; Oxford University: New York, 1987; Chapter 6.

(22) Teitelbaum, H.; Aker, P.; Sloan, J. J. *Chem. Phys.* **1988**, *119*, 79.

(23) Knutsen, K.; Dyer, M. J.; Copeland, R. A. *J. Chem. Phys.* **1996**, *104*, 5798.

(24) Chalamala, B. R.; Copeland, R. A. *J. Chem. Phys.* **1993**, *99*, 5807.

(25) Yardley, J. T. *Introduction to Molecular Energy Transfer*; Academic Press: New York, 1980.

(26) Jaffer, D. H.; Smith, I. W. M. *Faraday Discussions Chem. Soc.* **1979**, *67*, 212.

(27) Smith, I. W. M.; Williams, M. D. *J. Chem. Soc., Faraday Trans. 2* **1985**, *81*, 1849.

(28) Benson, S. *The Foundations of Chemical Kinetics*; R. E. Krieger: Malabar, 1982; Chapter 3.

(29) Shalashilin, D. V.; Michtchenko, A. V.; Umanskii, S. Ya.; Gershenzon, Yu. M. *J. Phys. Chem.* **1995**, *99*, 11627.

(30) Cannon, B. D.; Robertshaw, J. S.; Smith, I. W. M.; Williams, M. D. *Chem. Phys. Lett.* **1984**, *105*, 380.

(31) Smith, I. W. M.; Williams, M. D. *J. Chem. Soc., Faraday Trans. 2* **1986**, *82*, 1043.

(32) Dobbs, K. D.; Dixon, D. A.; Komornicki, A. *J. Chem. Phys.* **1993**, *98*, 8852.

(33) Basch, H.; Hoz, S. *J. Phys. Chem. A* **1997**, *101*, 4416.

(34) Copeland, R. A.; Jeffries, J. B.; Crosley, D. R. *Chem. Phys. Lett.* **1987**, *138*, 425.

(35) Kenner, R. D.; Rohrer, F.; Stuhl, F. *J. Phys. Chem.* **1989**, *93*, 7824.